Journal of Inorganic Biochemistry 104 (2010) 697–703

Contents lists available at ScienceDirect

Journal of Inorganic Biochemistry

journal homepage: www.elsevier.com/locate/jinorgbio

New insights in the DNA-$[Cr(phen)_2(dppz)]^{3+}$ binding and photocleavage properties by the complex with an intercalating ligand

Judith Toneatto [a], Rodolfo A. Boero [a], Guadalupe Lorenzatti [b], Ana M. Cabanillas [b], Gerardo A. Argüello [a,*]

[a] INFIQC-CONICET, Dpto. de Fisicoquímica, Facultad de Ciencias Químicas, Universidad Nacional de Córdoba, Ciudad Universitaria, 5000 Córdoba, Argentina
[b] CIBICI-CONICET, Dpto. de Bioquímica Clínica, Facultad de Ciencias Químicas, Universidad Nacional de Córdoba, Ciudad Universitaria, 5000 Córdoba, Argentina

ARTICLE INFO

Article history:
Received 28 December 2009
Received in revised form 25 February 2010
Accepted 26 February 2010
Available online 6 March 2010

Keywords:
Chromium Complex
Photosensitization
Intercalating ligand
DNA binding
DNA photocleavage
Bacterial transformation
Bacterial growth photoinhibition

ABSTRACT

Due to the key role of DNA in cell life and pathological processes, the design of specific chemical nucleases, DNA probes and alkylating agents is an important research area for the development of new therapeutic agents and tools in Biochemistry. Hence, the interaction of small molecules with DNA has attracted in particular a great deal of attention.

The aim of this study was to investigate the ability of $[Cr(phen)_2(dppz)]^{3+}$ to associate with DNA and to characterize it as photocleavage reagent for Photodynamic Therapy (PDT).

Chromium(III) complex $[Cr(phen)_2(dppz)]^{3+}$, (dppz = dipyridophenazine, phen = 1,10-phenanthroline), where dppz is a planar bidentate ligand with an extended π system, has been found to bind strongly to double strand oligonucleotides (*ds*-oligo) and plasmid DNA with intrinsic DNA binding constants, K_b, of $(3.9 \pm 0.3) \times 10^5\ M^{-1}$ and $(1.1 \pm 0.1) \times 10^5\ M^{-1}$, respectively. The binding properties to DNA were investigated by UV–visible (UV–Vis) absorption spectroscopy and electrophoretic studies. UV–Vis absorption data provide clearly that the chromium(III) complex interacts with DNA intercalatively. Competitive binding experiments show that the enhancement in the emission intensity of ethidium bromide (EthBr) in the presence of DNA was quenched by $[Cr(phen)_2(dppz)]^{3+}$, indicating that the Cr(III) complex displaces EthBr from its binding site in plasmid DNA. Moreover, $[Cr(phen)_2(dppz)]^{3+}$, non-covalently bound to DNA, promotes the photocleavage of plasmid DNA under 457 nm irradiation. We also found that the irradiated Cr(III)-plasmid DNA association is able to impair the transforming capacity of bacteria. These results provide evidence confirming the responsible and essential role of the excited state of $[Cr(phen)_2(dppz)]^{3+}$ for damaging the DNA structure. The combination of DNA, $[Cr(phen)_2(dppz)]^{3+}$ and light, is necessary to induce damage. In addition, assays of the photosensitization of transformed bacterial suspensions suggest that *Escherichia coli* may be photoinactivated by irradiation in the presence of $[Cr(phen)_2(dppz)]^{3+}$. In sum, our results allow us to postulate the $[Cr(phen)_2(dppz)]^{3+}$ complex as a very attractive candidate for DNA photocleavage with potential applications in Photodynamic Therapy (PDT).

1. Introduction

Due to the key role of DNA in cell life and pathological processes, the design of specific chemical nucleases, DNA probes and alkylating agents is an important research area for the development of new therapeutic agents and tools in Biochemistry. Hence, the interaction of small molecules with DNA has attracted particular great deal of attention [1]. The two most common non-covalent binding motifs for such systems are the groove binding [2–4] and intercalating modes [5,6]. Many therapeutic agents, particularly anticancer drugs, are known to bind DNA via these motifs, and the possibility of gene modulation by specific sequence binding of small molecules to DNA has also been explored [7,8].

Metal complexes, which bind to DNA, have been extensively studied by a number of research groups over the last years, centering on the understanding of the photophysics and photochemistry imposed through interaction with DNA [9–14]. The interaction of transition metal polypyridyl complexes with DNA has also drawn considerable attention, and whose interest stemmed from developing likely candidates such as photocleavage reagents [15]. These metal complexes are known to bind to DNA through a series of interactions, such as the π-stacking interaction associated with the intercalation of aromatic heterocyclic groups between the base pairs, hydrogen-bonding and/or Van der Waals interactions in the case of binding to the groove of DNA helix. In this last context, complexes containing the organic ligand dipyrido[3,2-a:2′,3′-c]-phenazine (dppz) (Fig. 1) have been studied, particularly $[Ru(bpy)_2(dppz)]^{2+}$ (bpy = 2,2′bipyridyl) and $[Ru(phen)_2(dppz)]^{2+}$ [16]. Within this framework, polypyridyl Cr(III) complexes are especially attractive compounds due to the fact that their excited-state redox potentials are larger than those of the

* Corresponding author. Fax: +54 351 4334188.
E-mail address: gerardoa@fcq.unc.edu.ar (G.A. Argüello).

0162-0134/$ – see front matter © 2010 Elsevier Inc. All rights reserved.
doi:10.1016/j.jinorgbio.2010.02.010

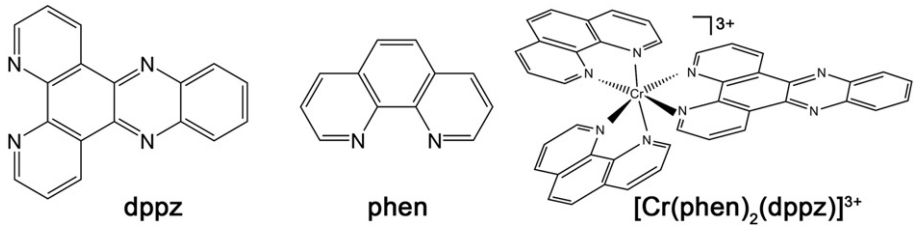

Fig. 1. Structure of the dipyrido[3,2-a:2′,3′-c]-phenazine (dppz) and 1, 10-phenanthroline (phen) used as ligands in the complex $[Cr(phen)_2(dppz)]^{3+}$.

analogous Ruthenium(II) complexes. For example, the redox potential of the excited state $[Ru(bpy)_3]^{2+}$ is 0.93 V. However, for analogous chromium complexes, the redox potential oscillates between 1.42 and 1.53 V that corresponds to $[Cr(phen)_2(dppz)]^{3+}$ (Fig. 1). This characteristic turns the complex into a better oxidant compound able to facilitate the Type I photosensitization mechanism. Interestingly, this mechanism for Cr(III) complexes makes this family of complexes potential photosensitizing agents for the treatment of hypoxic areas [17,18], offering a broad-range panel of biochemical applications, such as chemical photonucleases, photolyases and DNA chiral probes [19]. Although in this reference the photooxidation of deoxyguanosine-5′-monophosphe (dGMP) has been proved, at the molecular level of DNA, photodamage by Cr(III) diimines complexes has not yet been demonstrated. Nevertheless, the DNA photocleavage properties of Cr(III) complexes and DNA site-specific recognition continue to be an area of major interest.

In this work, we have used a planar bidentated ligand (dppz) coordinated to Cr(III) to test its binding properties to DNA, and to assess the ability and conditions of the Cr(III) complex ($[Cr(phen)_2(dppz)]^{3+}$) to impair the structure of DNA. UV–visible absorption spectroscopy and electrophoretic studies show that chromium(III) complex binds strongly to double strand oligonucleotides (*ds*-oligo) and plasmid DNA and interacts with DNA intercalatively. Competitive EthBr–Cr(III)complex binding experiments (EthBr=ethidium bromide) show that the Cr(III) complex displaces EthBr from its binding site in plasmid DNA. We also found that the irradiated Cr(III)-plasmid DNA is able to diminish the transforming capacity of bacteria. Moreover, the irradiation of bacteria, at specific wavelength, after its transformation with the Cr(III) complex-DNA showed a decrease in the number of colony forming units (CFU). Our results support a new role of $[Cr(phen)_2(dppz)]^{3+}$ as a photodamage reagent and its possible application in photodynamic therapy.

2. Materials and methods

2.1. Materials

The chromium (III) complex $[Cr(phen)_2(dppz)(CF_3SO_3)]_3$ was synthesized according to a previously reported procedure [20,21] with slight modifications. The stock solutions of $[Cr(phen)_2(dppz)]^{3+}$ were prepared in TRIS buffer (0.1 M Tris–HCl, 0.1 M NaCl, pH 7.4) and the concentration of chromium was calculated using molar absorptivity values of $\varepsilon_{360} = 13{,}900\ M^{-1}\ cm^{-1}$ [19]. All the experiments were carried out in TRIS buffer. Millipore Milli Q water (specific resistivity of 18.5 MΩ cm^{-1}) was used for preparing buffer solutions. All other chemical reagents were of analytical grade.

Subcloning vector pBS (pBluescript II SK(+), Genbank accession number x52328) and *Escherichia coli* XL1-Blue Subcloning-Grade Competent Cells were purchased from Stratagene (La Jolla, CA, USA). Molecular Weight Marker: λ DNA/EcoRI + Hind III Marker was purchased from Promega. The stock solution of Supercoiled (ccc form) and *Eco*RI-linearized (lin form) pBS were dissolved in 0.5x TE buffer (5 mM Tris–HCl, 0.5 mM EDTA pH 8 in MQ water), and kept at 4 °C and −20 °C respectively. The concentration of plasmid DNA per nucleotide was determined by absorption spectroscopy using the molar absorption coefficient (6600 $M^{-1}\,cm^{-1}$) at 260 nm [22]. The UV absorbance ratio of A_{260}/A_{280} was greater than 1.8, showing that the DNA was sufficiently free from protein [23].

Single strand oligonucleotides (*ss*-oligo) purchased from Sigma Genosys were annealed in annealing buffer (10 mM Tris pH 8, 50 mM NaCl, 1 mM EDTA pH 8) [23]. The sequences of the oligonucleotides were as follows: oligo A 5′ TCGACTCGCCAGTGCAAAGTAAGGTAGGTCTC-TACCCG -3, oligo B 5′ TCGACGGGTAGAGACCTACCTTACTTTGCACTGGC-GAG -3′. Single and double strand oligonucleotides (*ds*-oligo) were stored at −20 °C.

2.2. Instrumentation and methods

UV–visible (UV–Vis) spectra were obtained with an Agilent 8453 diode array detector spectrophotometer. Emission spectra were recorded on a Quanta Master QM2 Spectrofluorometer from PTI (Photon Technology International) equipped with a Hamamatsu R928 PMT in a photon counting detector.

2.3. DNA binding assays

The binding constant was determined by absorption titration of $[Cr(phen)_2(dppz)]^{3+}$ with either *ds*-oligo or plasmid DNA Supercoiled (ccc form). Electronic spectrum of $[Cr(phen)_2(dppz)]^{3+}$ was first recorded at concentration around 10^{-5} M, and subsequently, spectra of the same solution of the complex were recorded in the presence of increasing concentrations of DNA. Oligonucleotide concentrations ranged from 0 up to 2.6×10^{-6} M base pairs (bp) and Supercoiled plasmid DNA concentrations from 0 up to 5.7×10^{-5} M in bp. The intrinsic binding constants, K_b, were determined from the decrease in the absorbance at 360 nm with increasing concentrations of DNA by using Eq. (1) [24].

$$1/(\varepsilon_a - \varepsilon_f) = 1/(\varepsilon_b - \varepsilon_f) + 1/K_b(\varepsilon_b - \varepsilon_f)\,[DNA], \quad (1)$$

where ε_a, ε_f and ε_b are: the apparent absorption coefficient (absorbance/[Cr]), the extinction coefficient of the free complex, and the extinction coefficient of the bound complex, respectively. The values of K_b were obtained from the ratio of slope to the *y*-intercept, and the ε_b value could be extracted from the *y*-intercept.

2.4. Competitive binding experiments

To study the competitive binding of EthBr with Cr(III) complexes, EthBr was excited at 545 nm in the presence of plasmid DNA alone and in the presence of $[Cr(phen)_2(dppz)]^{3+}$ and $[Cr(phen)_3]^{3+}$. DNA was pretreated with EthBr in the ratio [DNA]/[EthBr] = 1 for 15 min at room temperature. Cr (III) complex concentrations (0 to 4.5×10^{-5} M) were then added to this mixture and the effect on the emission intensity was measured. The same experiment was repeated from a DNA solution pretreated with $[Cr(phen)_2(dppz)]^{3+}$ in the ratio [DNA]/[Cr(III)] = 1 for 15 min at room temperature. EthBr concentrations (0 to 3.3×10^{-5} M) were then added to this mixture and the effect on the emission intensity was measured.

2.5. Plasmid and bacteria photolysis

Test samples for photolysis purposes were prepared in sterile 0.6 ml tubes containing plasmid DNA (0.3 μg of pBS = pBluescript II SK(+)) with 240 μM chromium (III) complex to a final volume of 15 μL. The samples were irradiated with light of 457 nm. The source of irradiation was a white LED (type NSPW500CS, NICHIA America Corporation). The intensity of LED ($I_0 \sim 10^{-7}$ Einstein min^{-1}) was measured by actinometry using Potassium Ferrioxalate techniques [25]. For all the photolysis experiments, the irradiation beam was achieved with the LED attached in the cap of the tubes containing the photolysis solution. Where appropriate, deoxygenation was achieved by the passage of a stream of high purity N_2 over the 15 μL of the solutions at least for 10 h. Samples were kept at 6 °C under N_2 saturated or air-saturated atmosphere during irradiation, and stored in the dark before and after photolysis. The samples were loaded onto agarose gels after irradiation. The suspension transformed bacterial cells were photolyzed in the same conditions.

2.6. Agarose Gel electrophoresis

Photosensitized plasmid DNA samples were separated using horizontal 1% (w/v) agarose gel electrophoresis in 1xTAE buffer (40 mM Tris-acetate, 2 mM EDTA, pH 8.0). Electrophoresis was carried out at 100 V for 40 min to separate supercoiled covalently closed circular (ccc), open circular (oc), and linear (lin) forms of the plasmid DNA. After electrophoresis, DNA was visualized by soaking the gel for 15 min with an aqueous solution of ethidium bromide (0.5 μg/mL). The bands were seen in a transilluminator (254 nm) and the gel photographed to provide a record of the distances migrated by the various DNA fragments. The ratio of ccc to oc forms was estimated by densitometry using the WCIF ImageJ program.

2.7. Bacterial transformation of photosensitized plasmids

Transformations of *E. coli* XL1Blue strain were performed according to the manufacturer's protocol with 0.5 ng pBS plasmid DNA samples irradiated as indicated above. Following transformation, 100 μL bacterial suspensions were spread over the surfaces of Luria Broth agar plates in duplicate. For bacterial selection, plates contained 100 μg/mL Ampicillin (LB-Ampicillin Agar). The Petri dishes were incubated at 37 °C overnight. Transformed colonies were counted in order to ponderate the effect of irradiation on Cr(III)–DNA complex. All experimental procedures were performed at least three times.

2.8. Photoinactivation of transformed bacterial cells

Transformations of *E. coli* XL1Blue strain were performed with 0.5 ng pBS plasmid DNA and the appropriate concentration of Cr(III) complex (1×10^{-5} M) according to the manufacturer's protocol. Following transformation, 18 μL suspension of transformed bacterial cells in the presence of $[Cr(phen)_2(dppz)]^{3+}$ was irradiated with light of 457 nm. The irradiation was made in the same way as stated above. Samples were kept at 6 °C under air-saturated conditions during irradiation. After irradiation, the suspensions were diluted with 80 μL Super Optimal Broth (SOB medium) and 40 μl aliquots were spread over the surfaces of LB-Ampicillin Agar Petri dishes, in duplicate. The Petri dishes were incubated at 37 °C overnight. The colony forming units (CFU) were counted and a statistical analysis of the experimental data was performed using one-way analysis of variance (ANOVA) and Tukey test. The significance level was established at $p<0.05$.

3. Results and discussion

3.1. Characteristics of the binding $[Cr(phen)_2(dppz)]^{3+}$ to double strand intact DNA

Electronic absorption spectroscopy is one of the most useful techniques for DNA binding studies of metal complexes. The absorption spectrum of $[Cr(phen)_2(dppz)]^{3+}$ in aqueous buffer solution displays a low intensity shoulder of *d-d* origin at 430 nm, and an intense intraligand $\pi \rightarrow \pi^*$ absorption, characteristic of the dppz chromophore [26,27] in the 350–380 nm region. The absorption spectrum of the complex in the presence and absence of *ds*-oligo is depicted in inset Fig. 2. A clearly marked hypochromism in the dppz $\pi \rightarrow \pi^*$ transition, accompanied by an isosbestic point at 386 nm, was observed with the increase in *ds*-oligo concentrations. The same results were found when supercoiled plasmid DNA was used instead of *ds*-oligo (not shown). These spectral characteristics suggest a binding interaction between the complex and the DNA. A significant DNA perturbation of the dppz chromophore has been noted earlier for the same complex in the presence of increasing concentrations of calf thymus DNA [19].

The DNA-$[Cr(phen)_2(dppz)]^{3+}$ binding constants , K_b, were determined from the absorption data using Eq. (1). A plot of $1/(\varepsilon_a - \varepsilon_f)$ vs. 1/[*ds*-oligo] is shown in Fig. 2. The K_b values were $(3.9 \pm 0.3) \times 10^5$ M^{-1} for complex $[Cr(phen)_2(dppz)]^{3+}$-*ds*-oligo and $(1.1 \pm 0.1) \times 10^5$ M^{-1} for complex $[Cr(phen)_2(dppz)]^{3+}$-plasmid. In addition, from the *y*-intercept, the ε_b was estimated in $(5.8 \pm 0.3) \times 10^3$ $M^{-1}cm^{-1}$ and $(8.0 \pm 0.5) \times 10^3$ $M^{-1}cm^{-1}$ for the Cr(III) associated with *ds*-oligo and plasmid, respectively. The K_b slightly higher for the *ds*-oligo would indicate that, in the oligo, more base pairs should be available for the binding than in the supercoiled plasmid, and these binding constants are in accordance with the more lineal form of the calf thymus DNA previously reported [19]. These binding constant values indicate that $[Cr(phen)_2(dppz)]^{3+}$ binds more strongly to DNA than $[Cr(phen)_3]^{3+}$ whose binding constant is 3.5×10^3 M^{-1} [28,29]. Transition metallic complexes containing at least one intercalating ligand present binding constants in the order of 10^5–10^7 M^{-1}; the results obtained in the present work are consistent with those found in the literature for calf thymus [19,26] and suggest an intercalation model of dppz into the DNA bases. Since dppz possesses a greater planar area and extended π system than that of the phenanthroline

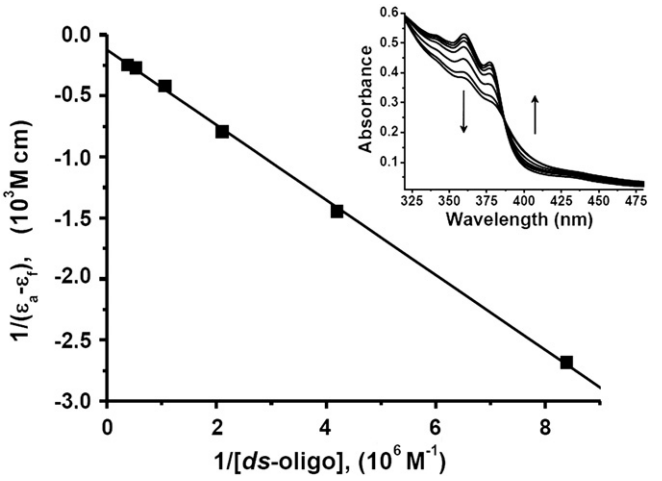

Fig. 2. The plot of $1/(\varepsilon_a - \varepsilon_f)$ vs 1/[*ds*-oligo] for $[Cr(phen)_2(dppz)]^{3+}$ 4.7×10^{-5} M in 100 mM of Tris–HCl buffer solution (pH 7.4) at 6 °C in the presence of increasing concentrations of *ds*-oligo (0, 1.2, 2.4, 4.7, 9.4, 19.0 and 26.0) $\times 10^{-7}$ M bases pair (bp); The correlation coefficient R = 0.999. *Inset*: Absorption spectra of chromium(III) complex at pH 7.4 in the presence of increasing concentrations of *ds*-oligo. Arrows show the absorbance changing upon the increase of *ds*-oligo concentration.

ligand, the former penetrates deeply and stacks strongly within the base pairs of DNA, while with the latter, the association involves the minor groove surface.

3.2. Cr(III) complex is able to displace EthBr from DNA

The competitive binding of the complexes and EthBr to DNA could provide valuable information on the nature of DNA binding to the chromium complex and its relative DNA binding affinity. In the presence of DNA, the emission intensity of EthBr is enhanced due to strong stacking interaction (intercalation) between the adjacent base pairs of DNA [30]. It was previously reported that the enhanced fluorescence can be quenched, at least partially, by the addition of a second intercalative molecule [31]. The quenching extents of fluorescence of EthBr bound to DNA are used to determine the relative DNA binding affinities of the second molecules. The emission spectra of EthBr and DNA-bound EthBr in the presence and absence of several concentrations of $[Cr(phen)_2(dppz)]^{3+}$ are shown in Fig. 3A. The addition of the Cr(III) complex to the DNA-bound EthBr solution caused a decrease in the emission intensity, indicating that the Cr(III) complex competitively bound to DNA and displaces the EthBr. Taking in account that the absorption bands of the chromium complex do not extend longer than 500 nm (inset of Fig. 2), at 545 nm (the experimental wavelength for the analysis of the competition binding study), no other process than the absorption of EthBr takes place. On the other hand, a similar experiment starting from $[Cr(phen)_2(dppz)]^{3+}$ pretreated with DNA and several aggregates of EthBr showed an improvement in emission intensity due to the displacement of DNA-bound Cr(III) complex by EthBr (Fig. 3B). In both experiments, when the concentration ratios of $[[Cr(phen)_2(dppz)]^{3+}]/[EthBr]$ attained 0.69, 50% of DNA-bound EthBr was replaced by $[Cr(phen)_2(dppz)]^{3+}$ and vice versa (Fig. 3C). Same experiments were done using $[Cr(phen)_3]^{3+}$ where no intercalating ligand was present.

Fig. 3C clearly shows that, in the same experimental condition, EthBr was slightly displaced by $Cr(phen)_3^{3+}$ compared with $[Cr(phen)_2(dppz)]^{3+}$. These results suggest that $[Cr(phen)_2(dppz)]^{3+}$ binds tightly to plasmid DNA (according to the intercalation model), similar to EthBr. These observations are consistent with those obtained from changes in UV–visible absorption spectra (inset Fig. 2) (see above). These experiments also suggest that both, the binding constant for the EthBr and the $[Cr(phen)_2(dppz)]^{3+}$ to DNA are within the same order of magnitude.

3.3. Cr(III) complex produces changes in the electrophoretic mobility of plasmid DNA

The effect of binding of $[Cr(phen)_2(dppz)]^{3+}$ to plasmid DNA was also confirmed by the ability of this compound to produce changes in the electrophoretic mobility of the supercoiled (ccc), open circular (oc) and linear (lin) form of plasmid DNA. The changes in the migration may be due to alterations in either: i) the mass, ii) the relative charge, and/or iii) the shape of the ccc form of the plasmid in the Cr(III)-DNA complex. Experiments with ccc, oc and lin forms of DNA were carried out. Fig. 4A shows the electrophoretic mobility pattern of native (~80% ccc to ~20% oc) pBS DNA (lane 1) and native pBS DNA incubated at increasing molar ratios (r_i) of $[Cr(phen)_2(dppz)]^{3+}$ per nucleotide, from $r_i = 0.0002$ to $r_i = 4$ (lanes 2 to 6). Fig. 4B shows the electrophoretic mobility pattern of lin form DNA (lane 2) incubated at increasing molar ratios (r_i) of $[Cr(phen)_2(dppz)]^{3+}$ per nucleotide, from $r_i = 0.0002$ to $r_i = 4$ (lanes 3 to 7), and DNA molecular weight marker (lane 1). The electrophoretic mobility of the ccc, oc and lin form gradually decreases as r_i increases relative to the control (without complex), suggesting that the plasmid DNA runs associated with the Cr(III) complex. The lower mobility of DNA could result from the converging effects mentioned above; Cr(III) complex is able to electroneutralizar the negative charges of DNA backbone and also to increase the mass of the running DNA.

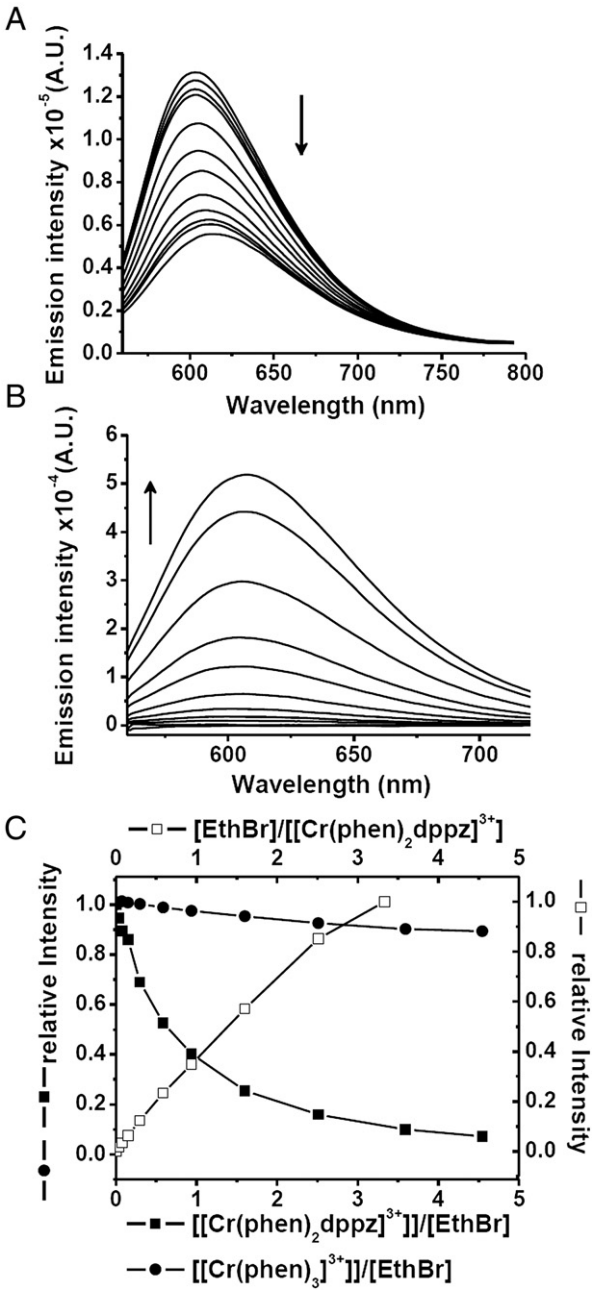

Fig. 3. The competitive binding of the Cr(III) complexes and EthBr to DNA. A: Changes in the emission spectra of EthBr (1×10^{-5} M) in the absence of plasmid DNA (bottom line), and in the presence of plasmid DNA (1×10^{-5} M per nucleotide) with increasing concentrations of $[Cr(phen)_2(dppz)]^{3+}$ (0, 0.38, 0.75, 1.50, 3.00, 5.90, 9.40, 16.0, 25.0, 36.0 and 45.0) $\times10^{-6}$ M (from top to bottom). B: Increase in the emission intensity of EthBr bound to DNA. The starting conditions are $[Cr(phen)_2(dppz)]^{3+}$ (1×10^{-5} M) in the presence of plasmid DNA (1×10^{-5} M per nucleotide) and in the absence of EthBr (bottom line), with increasing concentrations of EthBr (0, 0.38, 0.75, 1.50, 3.00, 5.90, 9.40, 16.0, 25.0 and 33.0) $\times10^{-6}$ (from bottom to top). C: Plot of relative intensity of EthBr-DNA complex (I/I_0) vs. [Cr(III)]/[EthBr] or [EthBr]/[Cr(III)]. $[Cr(phen)_2(dppz)]^{3+}$ (-■-),$[Cr(phen)_3]^{3+}$ (-●-) and [EthBr] (-□-).

Although it is difficult to determine what is the major effect, i.e., charge or mass, it is clear that both are present. An alternative explanation is that the intercalation could be distorting the degree of supercoiling and therefore changing shape of the DNA. However, the effect of binding of Cr(III) complex to the linearized form of plasmid DNA seems to rule out this possibility since a similar delay was found in both DNA forms closed circular and relaxed (lin). So that, conformational changes seem to be negligible in the delay of the ccc band in front of the other two effects.

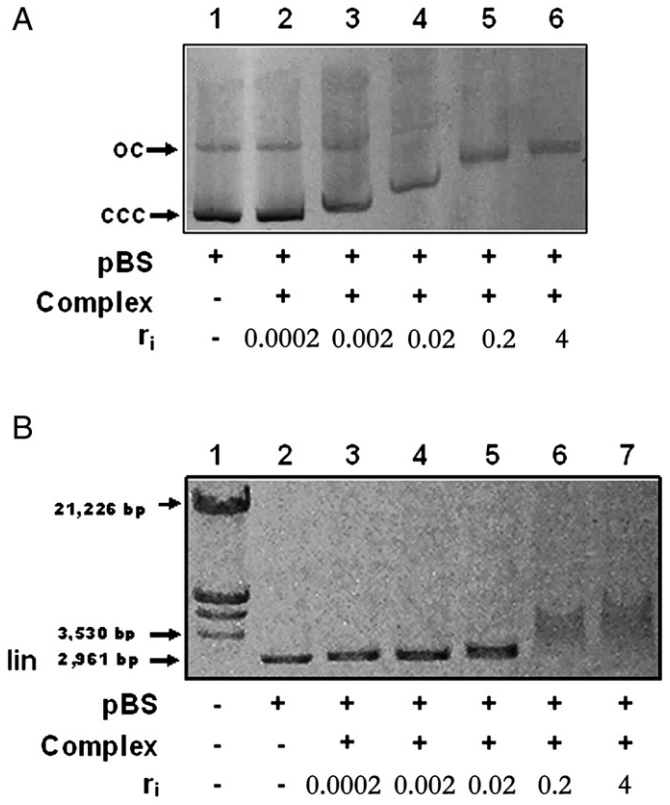

Fig. 4. A: Agarose gel (1%) electrophoresis showing changes in electrophoretic mobility of the oc and ccc forms of pBS plasmid incubated for 12 h at 6 °C with different $[Cr(phen)_2(dppz)]^{3+}$ concentrations: lane 1, pBS DNA in the absence of complex (control), lanes 2 to 6, pBS incubated at increasing molar ratios of $[Cr(phen)_2(dppz)]^{3+}$ per nucleotide, r_i of 0.0002, 0.002, 0.02, 0.2 and 4, respectively. B: Agarose gel (1%) electrophoresis showing changes in electrophoretic mobility of the lin form of pBS plasmid incubated for 12 h at 6 °C with various $[Cr(phen)_2(dppz)]^{3+}$ concentrations: lane 1, DNA Molecular Weight Marker, lane 2, control lin form pBS DNA, lanes 3 to 7, lin form pBS incubated at increasing molar ratios of $[Cr(phen)_2(dppz)]^{3+}$ per nucleotide, r_i of 0.0002, 0.002, 0.02, 0.2 and 4, respectively.

In addition, and in agreement with the results found in the competitive binding study (Fig. 3), the intensity of the bands decreases from lanes 1 to 6 in Fig. 4A and lanes 2 to 7 in Fig. 4B due to the competition between the EthBr and $[Cr(phen)_2(dppz)]^{3+}$ for the binding to DNA.

3.4. Photo-induces cleavage in plasmid DNA

Photodynamic therapy (PDT) is a technique that uses light activated photosensitizers, i.e. compounds that are nontoxic until irradiated with light of an appropriate wavelength tuned to the absorption band of the photosensitizer. It is important to emphasize that the relationship between the wavelength emitted by the light source and the absorption spectra of the photosensitizer is essential to cause photochemical and photophysical effects. In photodynamic therapy, a close relationship between the absorption of the complex and the wavelength should be observed. Thus, toxicity in the cell only occurs when the wavelength of the radiation emitted by the source is under the absorption band of the photosensitizer. All Together, the light wavelength, photosensitizer absorbance, light intensity and exposure time play a decisive role in the results since, to achieve the best effects, the photosensitizer has to be efficiently sensitized by the light source.

The photodynamic activity of the photosensitizer is based on photooxidative reactions, which induce multiple consecutive biochemical and morphological reactions. When a photosensitizer molecule absorbs, it can undergo an electronic transition to the singlet excited state, a short-lived excited state which could be converted into a long-lived triplet state via an intersystem crossing process. This triplet state or photoactive state can generate cytotoxic species like singlet oxygen. These reactive oxygen species are responsible for irreversible damage to cell membranes, including protein modifications. Nevertheless, polypyridyl Cr(III) complexes may be expected to develop their photodamaging effects primarily via the photosensitization mechanism Type I (direct photooxidation of the substrate), with minor contribution from the classical Type II mechanism (indirect via singlet oxygen formation). Interestingly, the mechanism for these complexes makes this family potential photosensitizing agent for the treatment of hypoxic areas [17,18].

There is a particular ongoing interest in DNA cleavage reactions photoactivated by metal complexes [15,32]. The cleavage reaction on plasmid DNA can be monitored by agarose gel electrophoresis. When circular plasmid DNA is subject to electrophoresis, a relatively fast migration is observed in the intact supercoiled ccc form. If a break occurs on one strand (nicking), the supercoiled structure of DNA will relax to generate a slower-moving oc form. If both strands are cleaved, a lin form will be generated and will migrate between ccc and oc forms [33].

In order to assess whether $[Cr(phen)_2(dppz)]^{3+}$ induces damage in the plasmid DNA as a result of irradiation, agarose gel electrophoresis were performed. Fig. 5 shows gel electrophoretic separations of plasmid DNA after incubation with and without $[Cr(phen)_2(dppz)]^{3+}$ at different irradiation times. The concentration of Cr(III) complex and plasmid DNA used in the experiment correspond to $r_i = 4$. As

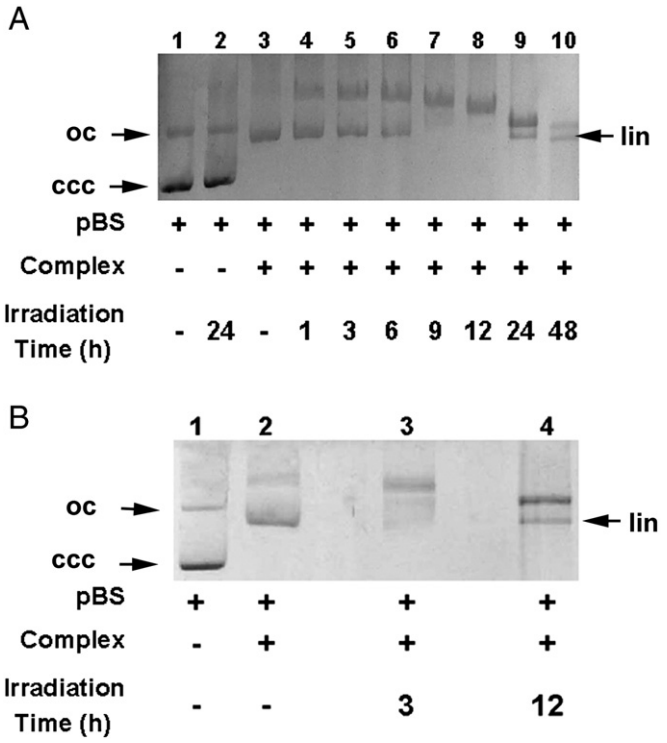

Fig. 5. A: Agarose gel (1%) electrophoresis showing the DNA photocleavage induced by 2.4×10^{-4} M $[Cr(phen)_2(dppz)]^{3+}$ at different irradiation times at 6 °C in the presence of air-saturated atmosphere in 100 mM of Tris–HCl buffer (pH 7.4): Lane 1, control pBS DNA non-irradiated; Lane 2, DNA irradiated for 24 h in the absence of Cr(III) complex; Lane 3, DNA + Cr(III) complex non-irradiated; Lanes 4 to 10, DNA + Cr(III) complex with irradiation times of 1, 3, 6, 9, 12, 24 and 48 h respectively. B: same conditions as A: in the absence of oxygen Lane 1, control pBS DNA non-irradiated; Lane 2, DNA + Cr(III) complex non-irradiated; Lanes 3 and 4, DNA + Cr(III) complex with irradiation times of 3 and 12 h, respectively.

indicated in Fig. 5A, the control plasmid DNA (pBS) (lane 1) contains ~80% ccc form and ~20% oc form. In the presence of Cr(III) complex and in agreement with Fig. 4, DNA ccc and oc forms run more cathodic, thus lanes 3 to 10 are slower than lines 1 and 2. As observed, from lanes 4 to 10 the Cr(III) complex induces a decrease in the amount of the ccc form, whereas the oc form increases with the irradiation time. Furthermore, an increase in the intensity and mobility of the oc band is observed. A pattern compatible with a DNA lin form is shown in lanes 9 and 10 corresponding to 24 and 48 h of irradiation time, respectively. The presence of chromium alone does not cause significant changes in (lane 3) the DNA ccc:oc ratio. In addition, the mere presence of light in the absence of Cr(III) complex does not modify plasmid DNA mobility, even at the longest irradiation time (lane 2). From lanes 3 to 6 the results were as expected and discussed above. In lane 7 the ccc band disappears and starts to increase the mobility of the oc form as well as its intensity up to lane 9, where a new band with higher mobility appears which was attributed to the lin form. The oc form increases mobility and intensity due to the fact that in the photooxidation reaction the complex is released from the plasmid. In consequence, the oc form becomes lighter than oc-Cr(III) increasing its mobility. Its intensity also increases because the EthBr occupy the sites left by the Cr(III) complex. As can be seen in lane 10 (Fig 5A), the effect of photodamage is especially marked at longer irradiation times, where practically all the bands begin to disappear.

The same experiment was repeated in N_2 saturated atmosphere (negligible oxygen levels). Fig. 5B shows gel electrophoretic separations of plasmid DNA after incubation with $[Cr(phen)_2(dppz)]^{3+}$ at different irradiation times, 3 h and 12 h. The control plasmid DNA (lane 1) contains ~80% DNA ccc form and ~20% DNA oc form; in the presence of Cr(III) complex and without irradiation, the same ratio ccc/oc is maintained (lane 2). However, the amount of oc form increases, whereas the amount of ccc form decreases as the irradiation time increases (lanes 3 and 4). A pattern compatible with a DNA lin form after 12 h of irradiation is shown in lane 4.

These results suggest that the excited states of $^*[Cr(phen)_2(dppz)]^{3+}$ are responsible for the cleavage observed. The combination of DNA, $[Cr(phen)_2(dppz)]^{3+}$ and light is necessary and sufficient to produce damage to the DNA structure. Moreover, the efficiency of cleavage in the absence of oxygen is higher than in the presence of oxygen indicating that the direct photooxidation (Type I) mechanism is the responsible for the changes observed. Indeed, the photocleavage ability correlates fairly well with the oxidation power of the excited state of $[Cr(phen)_2(dppz)]^{3+}$, which is capable of oxidizing the guanine and adenine nucleobases [19].

3.5. Photosensitization impairs transforming ability of the plasmid DNA

To show if the damage generated in the plasmid DNA by irradiation in the presence of $[Cr(phen)_2(dppz)]^{3+}$ induces modifications in the viability of living cells, we have developed an assay relating the DNA integrity to the number of transformed bacterial colonies with plasmid DNA. Thus, the XL1Blue strain of *E. coli*, which is unable to grow in an ampicillin agar plate, is transformed by the incorporation of a plasmid DNA (pBS) that carries an ampicillin resistance cassette. The number of transformed colonies is proportional to the integrity of the plasmid DNA. Competent *E. coli* XL1Blue bacteria cells were transformed with irradiated and non-irradiated pBS plasmid DNA and the corresponding controls were run. The time of photolysis ranged from 1 to 24 h. As expected, the number of colonies decreased dramatically when the bacteria incorporated the photosensitized plasmid in the presence of Cr(III) complex, as depicted in Fig. 6A. The longer the irradiation time, the higher the bacterial growth inhibition achieved. An inhibition higher than 98% was reached at short times of light treatment such as 3 h. The controls (bars 1, 2 and 3) showed that the presence of both, complex and light was required to induce DNA damage (Fig. 6A).

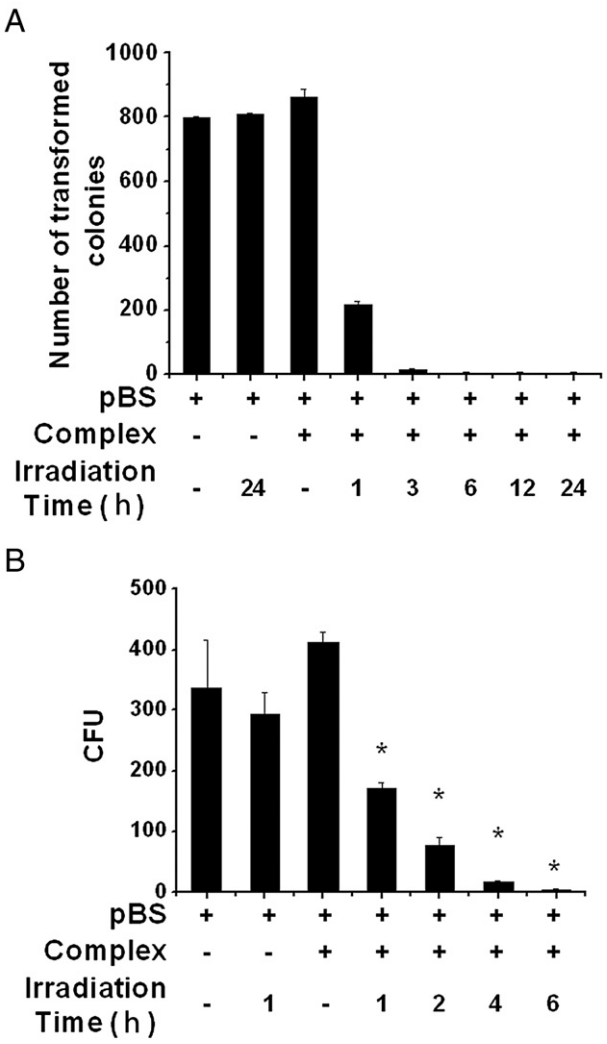

Fig. 6. A: Plot showing the number of transformed colonies with DNA irradiated in the presence of $[Cr(phen)_2(dppz)]^{3+}$: bar 1, control number of colonies transformed with non-irradiated pBS DNA; bar 2, number of colonies transformed with pBS DNA irradiated for 24 h in the absence of Cr(III) complex; bar 3, number of colonies transformed with pBS DNA + Cr(III) complex non-irradiated; bars 4 to 8, number of colonies transformed with pBS DNA + Cr(III) complex with irradiation times of 1, 3, 6, 12 and 24 h, respectively. Values represent an average of three different experiments ± standard deviation of the mean (σ/N). B: Figure represents the number of viable *E. coli* XL1Blue bacteria cells transformed with pBS plasmid. bar 1, control bacterial suspension (untreated); bar 2, bacterial suspension irradiated for 1 h in the absence of Cr(III) complex; bar 3, non-irradiated bacterial suspension treated with Cr(III) complex; bars 4 to 7, bacterial suspension treated with Cr(III) complex and irradiated for 1, 2, 4 and 6 h , respectively. Values represent an average of four different experiments ± standard deviation of the mean (σ/N). Means were compared by ANOVA followed by Tukey test. $^*p<0.05$.

3.6. Photoinactivation of transformed bacterial cells

We also performed an alternative approach to assess the effects of photoirradiation to bacterial cells as a model of living cells. For these experiments, we first transformed *E. coli* XL1Blue bacteria cells with pBS plasmid in the presence of the Cr(III) complex solutions, which was followed by irradiation. The colonies were counted and statistically analyzed. The results are shown in Fig. 6B. A substantial death of cells was obtained on irradiation with light at $\lambda = 457$ nm in the presence of $[Cr(phen)_2(dppz)]^{3+}$. An inhibition higher than 60% was reached at short times of light treatment such as 1 h, achieving a complete inhibition at 6 h. Statistically significant differences were observed among the varying irradiation times ($p<0.05$). The controls showed that light (bar 2) and Cr(III) complex (bar 3) alone were not able to induce

bacterial inactivation (Fig. 6B). Thus, $[Cr(phen)_2(dppz)]^{3+}$ brings about inhibition of bacterial growth only in the presence of light.

4. Concluding remarks

In this work we show that $[Cr(phen)_2(dppz)]^{3+}$ intercalates as homologous Ruthenium complexes do [16]. In this sense, we describe novel properties of $[Cr(phen)_2(dppz)]^{3+}$. i) First, we demonstrated the ability of this complex to occupy EthBr's binding sites; ii) the Cr(III) complex was able to interact with the DNA inducing DNA damage after reaching its excited state; and iii) the irradiation of transformed bacteria in the presence of $[Cr(phen)_2(dppz)]^{3+}$ caused a strong photoinactivation of the viable cells decreasing significantly the number of bacterial colonies at short exposure times. Even though here we have studied the Cr(III) complex ability to cause DNA photoclevage and cellular photoinactivation, we still need to address further investigations in order to obtain more information on the biological effects of this agent. These distinctive attributes suggest that $[Cr(phen)_2(dppz)]^{3+}$ may act as a new reagent in photodynamic therapy.

Acknowledgments

The authors (G.A.A. and A.M.C.) thank Consejo Nacional de Investigaciones Científicas y Técnicas de Argentina (CONICET), Secretaría de Ciencia y Técnica de la Universidad Nacional de Córdoba (SECyT) and Agencia Nacional de Promoción de la Ciencia y Técnica (ANPCYT) for financial support. J. T. and G. L. are research fellows from CONICET. G. A. A. and A. M. C. are researchers from CONICET.

References

[1] D.S. Johnson, D.L. Boger, DNA Binding Agents, in: J.L. Atwood, J.E.D. Davies, D.D. MacNicol, F. Vögtle (Eds.), Comprehensive Supramolecular Chemistry, vol. 4, Pergamon, Oxford, 1996.
[2] C. Zimmer, U. Wahnert, Prog. Biophys. Mol. Biol. 47 (1986) 31–112.
[3] N.T. Thong, C. Hélène, Angew. Chem. Int. Ed. Engl. 32 (1993) 666–689.
[4] P.B. Dervan, B.S. Edelson, Curr. Opin. Struct. Biol. 13 (2003) 284–299.
[5] L.P.G. Wakelin, Polyfunctional Med. Res. Rev. 6 (1986) 275–340.
[6] B.H. Geierstanger, D.E. Wemmer, Annu. Rev. Biophys. Biomol. Struct. 24 (1995) 463–493.
[7] M. Faria, C.D. Wood, L. Perrouault, J.S. Nelson, A. Winter, M.R.H. White, C. Hélène, C. Giovannangeli, Proc. Natl. Acad. Sci. U.S.A. 97 (2000) 3862–3867.
[8] J.M. Gottesfeld, L. Neely, J.W. Trauger, E.E. Baird, P.B. Dervan, Nature 387 (1997) 202–205.
[9] S.J. Lippard, Acc. Chem. Res. 11 (1978) 211–217.
[10] D.S. Sigman, T.W. Bruice, A. Mazumder, C.L. Sutton, Acc. Chem. Res. 26 (1993) 98.
[11] B. Nordén, P. Lincoln, B. Akerman, E. Tuite, DNA interactions with substitution-inert transition metal ion complexes, in: H. Sigel, A. Sigel (Eds.), Metal ions in biological systems, vol. 33, Marcel Dekker, New York, 1996, p. 177.
[12] K.E. Erkkila, D.T. Odum, J.K. Barton, Chem. Rev. 99 (1999) 2777–2795.
[13] C. Metcalfe, J.A. Thomas, Chem. Soc. Rev. 32 (2003) 214–215.
[14] A.K.-D. Mesmaeker, J.P. Lecomte, J.M. Kelly, Top. Curr. Chem. 177 (1996) 25–76.
[15] B. Elias, A.K.-D. Mesmaeker, Coord. Chem. Rev. 250 (2006) 1627–1641.
[16] A.E. Friedman, J.-C. Chambron, J.-P. Sauvage, N.J. Turro, J.K. Barton, J. Am. Chem. Soc. 112 (1990) 4960–4962.
[17] C.S. Foote, Science 162 (1968) 963–970.
[18] D. Pagliero, G.A. Argüello, E.H. Staricco, J. Photochem. Photobiol. A: Chem. 115 (1998) 199–206.
[19] K.D. Barker, B.R. Benoit, J.A. Bordelon, R.J. Davis, A.S. Delmas, O.V. Mytykh, J.T. Petty, J.F. Wheeler, N.A.P. Kane-Maguire, Inorg. Chim. Acta 322 (2001) 74–78.
[20] J.E. Dickenson, L.A. Summers, Aust. J. Chem. 23 (1970) 1023.
[21] K.D. Barker, K.A. Barnett, S.M. Connell, J.W. Glaeser, A.M. Wallace, J. Wildsmith, B.J. Herbert, J.F. Wheeler, N.A.P. Kane-Maguire, Inorg. Chem. Acta 316 (2001) 41–49.
[22] M.E. Reichmann, S.A. Rice, C.A. Thomas, P.A. Doty, J. Am. Chem. Soc. 76 (1954) 3047–3053.
[23] J. Marmur, J. Mol. Biol. 3 (1961) 208–211.
[24] A. Wolfe, G.H. Shimer, T. Meehan, Biochemistry 26 (1987) 6392–6396.
[25] S.L. Murov, Handbook of Photochemistry, Actinometry, Section 13, Marcel Dekker inc, New York, 1973, pp. 119–128.
[26] C. Hiort, P. Lincoln, B. Nordén, J. Am. Chem. Soc. 115 (1993) 3448–3454.
[27] R.E. Holmlin, J.A. Yao, J.K. Barton, Inorg. Chem. 38 (1999) 174–189.
[28] R.T. Watson, N. Desai, J. Wildsmith, J.F. Wheeler, N.A.P. Kane-Maguire, Inorg. Chem. 38 (1999) 2683–2688.
[29] R. Vijayalakshmi, M. Kanthimathi, V. Subramanian, B.U. Nair, Biochim. Biophys. Acta 1475 (2000) 157–162.
[30] J.B. LePecq, C. Paoletti, J. Mol. Biol. 27 (1967) 87–106.
[31] B.C. Baguley, M. Le Bret, Biochemistry 23 (1984) 937–943.
[32] B. Armitage, Chem. Rev. 98 (1998) 1171–1200.
[33] J.K. Barton, A.L. Raphael, J. Am. Chem. Soc. 106 (1984) 2466–2468.